

We are IntechOpen, the world's leading publisher of Open Access books Built by scientists, for scientists

6,900

Open access books available

186,000

International authors and editors

200M

Downloads

Our authors are among the

154

Countries delivered to

TOP 1%

most cited scientists

12.2%

Contributors from top 500 universities



WEB OF SCIENCE™

Selection of our books indexed in the Book Citation Index
in Web of Science™ Core Collection (BKCI)

Interested in publishing with us?
Contact book.department@intechopen.com

Numbers displayed above are based on latest data collected.
For more information visit www.intechopen.com



Dendrimers as Dopant Atom Carriers

Haigang Wu and Yaping Dan

Additional information is available at the end of the chapter

<http://dx.doi.org/10.5772/intechopen.71397>

Abstract

Properties of modern semiconducting transistors and future electron or quantum devices are essentially determined by single dopant atoms. How to precisely control the individual dopant position is one of the key factors to advance these technologies. In this chapter, we first briefly introduce the research progress in single dopant devices. To fabricate single dopant devices at large scale, we then overview our previous propose to control the locations of single dopants by self-assembly of large molecules (polyglycerols) with each carrying one dopant atom. The synthesis process, doping properties, and challenges of the molecular doping technique will be thoroughly elaborated before we conclude this chapter.

Keywords: monolayer doping, dendrimer, dopant carriers, hyperbranched polyglycerols

1. Introduction

Dopants play an important role in electrical [1], optical [2], and other properties [3] of semiconductors. As the size of semiconducting devices scales down, the device functionality will be essentially determined by the property of a single dopant atom. In recent years, these single atom devices such as single atom transistors [4] and atomic memory devices [5] have been demonstrated. The technology that can place dopants precisely at arbitrary locations is the key to electronics based on single dopant atoms. Although single atom devices have not commercialized, the precise control of dopant locations is still important to today's integrated circuits. For example, an ordered array of dopants in the channel of metal-oxide-semiconductor field-effect transistors (MOSFET) will help suppress the fluctuation of threshold voltage [6–8].

In 2005, Shinada et al. [6] reported that transistors based on uniformly distributed dopants were successfully developed by single ion implantation (SII) technique in which individual

ions were controlled by chopping a focused ion beam through an aperture. With this technique, a broad range of single ions such as B, Si, and P can be controlled individually. Indeed, for transistors based on dopants that are spatially distributed at a uniform pattern, the fluctuation of threshold voltages is significantly suppressed, compared to those based on randomly distributed dopants by traditional ion implantation. In the meantime, an Australian research group developed a new “hydrogen lithography” technique to control single dopants. In 2012, this group first reported transistors based on a single P dopant atom. The “hydrogen-lithography” technique is based on the removal of single hydrogen atom on the Si-H surface by scanning tunneling microscopy (STM). A single phosphine molecule will be self-assembled onto the Si dangling bond after the hydrogen is removed. In the end, the P atoms will be diffused into the Si substrate by thermal annealing. Transistors based on single P atoms were fabricated and investigated. In addition, resistors based on a line of P dopants were also characterized, showing that the Ohm’s law is still effective at atomic level [9].

However, these single dopant control techniques are time-consuming serial processes and will be inefficient for industry applications. How to control individual dopants at large scale is urgently needed for future electronics based on single dopant atoms. We previously proposed to control individual dopants at large scale by the self-assembly of molecules with each carrying one dopant atom [10]. The substrate surface is patterned chemically by advanced lithography so that the carrier molecules will be grafted onto the desired locations as designed. Due to the limitation of the today’s advanced lithography, the surface patterns are on an order of 10 nm. Multiple molecules will be grafted onto each patterned area unless the molecule size is comparable to the surface pattern size. Clearly, large molecule carriers are required to control single dopants at large scale.

Dendrimers are a series of large molecules, the size of which can be controlled during synthesis. We previously synthesized dendrimers with a diameter of more than 10 nm [10]. Each dendrimer carries only one P dopant. These dendrimers as dopant carriers can be self-assembled on the substrate. The dopants will be driven into silicon to form electrically active dopants by thermal annealing. Although the dopants will diffuse in all directions during the annealing process, the rapid thermal annealing and other techniques, such as laser-based annealing process can limit the dopants in the ultra-shallow surface. In short, the dendrimer-based monolayer doping technique is potentially a promising approach to control individual dopants at large scale. This chapter is to review the potential application of dendrimers as single dopant carriers.

2. Atom control and devices design

As reported [6], deterministic dopants help suppress the fluctuation of threshold voltages in CMOS field-effect transistors. More importantly, individual dopant-related devices are also the frontier in the microelectronic field. For example, single atom transistor and single magnetic atom memory were demonstrated. In this section, we will briefly overview the single atom devices and related properties.

Xie *et al.* [11] firstly reported a single atom transistor (**Figure 1**) based on redox circles of the electrochemistry. To fabricate the device, a pair of Ag electrodes was etched to be in contact via a single Ag atom using AgNO_3 and HNO_3 mixture as the electrolyte. When the single Ag atom

contact was electrochemically oxidized, the circuitry would be in “off” state. As a reverse process, the circuitry can be in “on” state by reduction. Besides silver, Pb can be also made to single atom transistors by a similar method [12]. Moreover, Martin *et al.* [13] used the elastic properties of single atom relays and substrates to control single-atom switch in which the gate voltage can be performed to regulate the switch “on-off” state between the monatomic contact condition and the tunneling regime state. These works opened a new horizon to investigate atomic level switches, although the devices were made in electrolyte solution. However, one critical shortage of monatomic contact-based transistor is the poor stability and repeatability of single atom contact in the “on-off” circles, which is of significant impact on the development and application in industry.

In 1998, Kane proposed [14] a new architecture of spin transistors made of single P atoms in silicon substrate (**Figure 2**), based on the well-developed Si:³¹P system in the past four decades. As known in semiconductor physics, phosphorus dopants as a donor-type of dopants in Si will provide free electrons with the wavefunction spreading out in the crystal lattice. The electron wave function of one P donor is also easily affected by the nuclear spin of another P donor. This nuclear-nuclear spin interaction mediated by electrons can be employed as an excellent approach to control the logical operation, because these hyperfine interactions can be controlled by gate voltages [15]. For the purified ²⁸Si isotope bulk with P-doping, the outer electron of ³¹P at low temperature (1.5 K) is unionized, and it can be ionized by external electric field, for example, metallic gate voltage. When ³¹P donor is under positive charge with 1/2 nuclear spin, the interaction range of electron wave function can extend tens of nanometers away from ionized phosphorus nucleus, and the electron-mediated nuclear spin coupling can be observed by using electron spin-resonance spectroscopy (ESR). To perform this type of quantum calculations, there are three necessary parameters: modulation of the hyperfine interaction length by gate voltage, control of “on-off” states for single donor, and the resonance flipping of nuclear spins by global magnetic field. Pla *et al.* [16] reported the readout and control of ³¹P spin in Si with 99.8% fidelity. Vrijen *et al.* [17] presented in their work that Si/Ge epitaxial heterostructures were selected to control the single-phosphorus electron spin. Morton *et al.* [18] demonstrated a quantum memory by using ³¹P nuclear spin. However, the most important obstacle of spin-based quantum computers is the short coherent time (less than 100 ms) at low temperature. It is caused by the ²⁹Si isotope and the environment effect. It still needs more work to explore and optimize the testing condition to achieve a long coherent and dephase time.

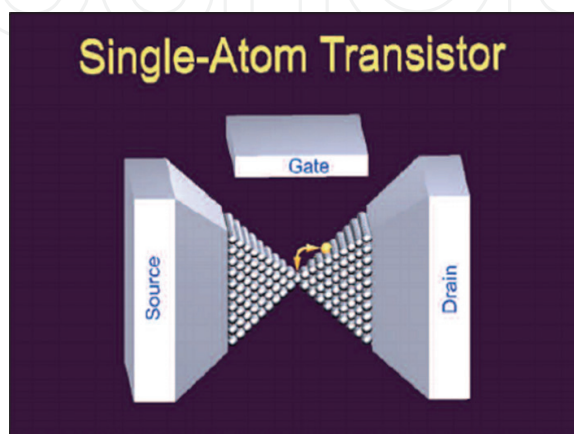


Figure 1. Single atom transistor to be as switch (Ref. 11).

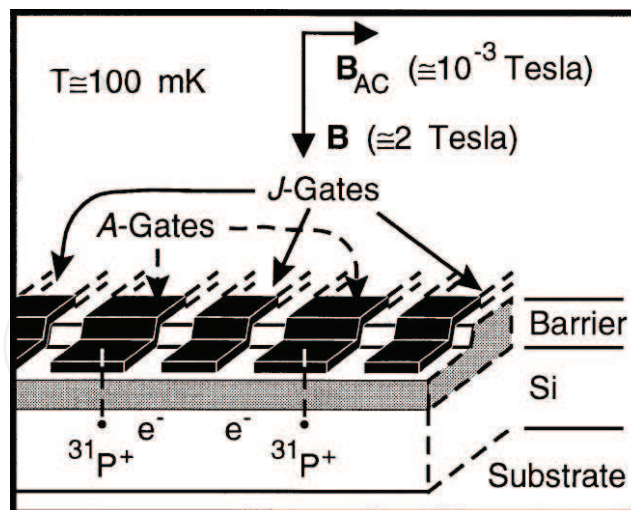


Figure 2. ^{31}P nuclear-spin-based single atom transistor (Ref. 14).

In the microelectronics industry, how to produce the large area density of bit information in memory devices is an important task [19]. Richard Feynman once said “all of the information that man has carefully accumulated in all the books in the world, can be written... in a cube of material one two-hundredth of an inch wide” [20]. He used the cubic array 125 atoms ($5 \times 5 \times 5$ array) to store the information (one bit) [21], which is comparable to the data storage in DNA (32 atoms for one bit). This sentence gives a glimpse into how to significantly improve the areal density of data storage down to atomic level. Afterward, using single molecules or nanotubes as basic unit to store information has been extensively explored, and the types of memory structures also have been extended to be more diversiform, for example, nanowire arrays [22]. However, the final goal of memory devices is to achieve the atomic level storage at room temperature [23]. To reach this goal, Feynman designed the atomic level memory bit structure [21], which is more efficient than classical CD-ROM storage as shown in Figure 3. These images were coded by Morse code, and this atomic level memory

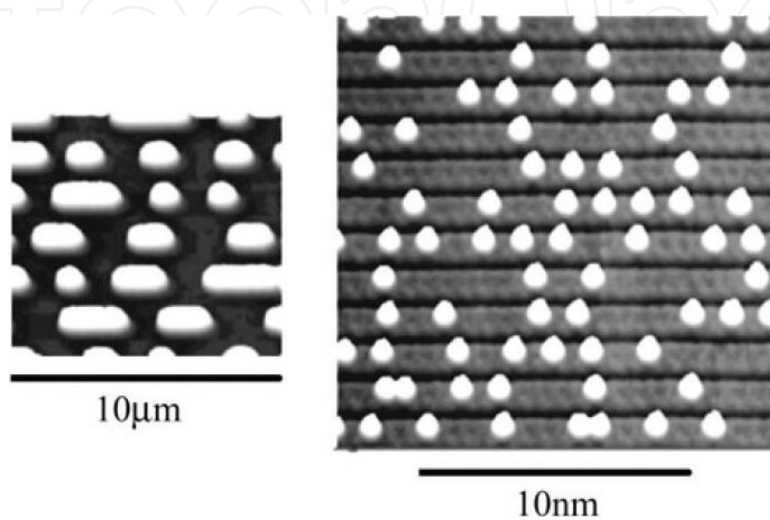


Figure 3. Comparison of atomic memory with CD-ROM (Ref. 21).

significantly improves the capacity for per area. To achieve this final goal, it is the key to develop a technology that can place individual dopants at specific sites at a large scale.

Recently, Kalff *et al.* [24] reported the kilobyte rewritten atomic memory devices. In their work, the chlorine self-assembled atomic layer was first prepared on the Cu(100) surface, and then scanning tunneling microscope (STM) was used to control the vacancy of chlorine on the copper surface. An array of 12×12 atoms as the basic memory unit was created, and the ASCII code was used to encode the characters on the copper surface. These memory units can operate at 77 K, and were used to write the Feynman's lecture "There's plenty of room at the bottom." The authors successfully used the vacancy of atoms to encode the byte information, and the memory volume is significantly improved to 1016 bytes, the area density of which achieved to $0.778 \text{ bits nm}^{-1}$. Moreover, Schirm *et al.* [23] reported the current-driven single atom memory by changing the "on-off" state to code the information. Maze *et al.* [25] demonstrated the individual electronic spin state in the diamond to code information. Clearly, the fabrication of atomic memory devices needs the precise control of the atom positions to code information bit by bit (**Figure 4**).

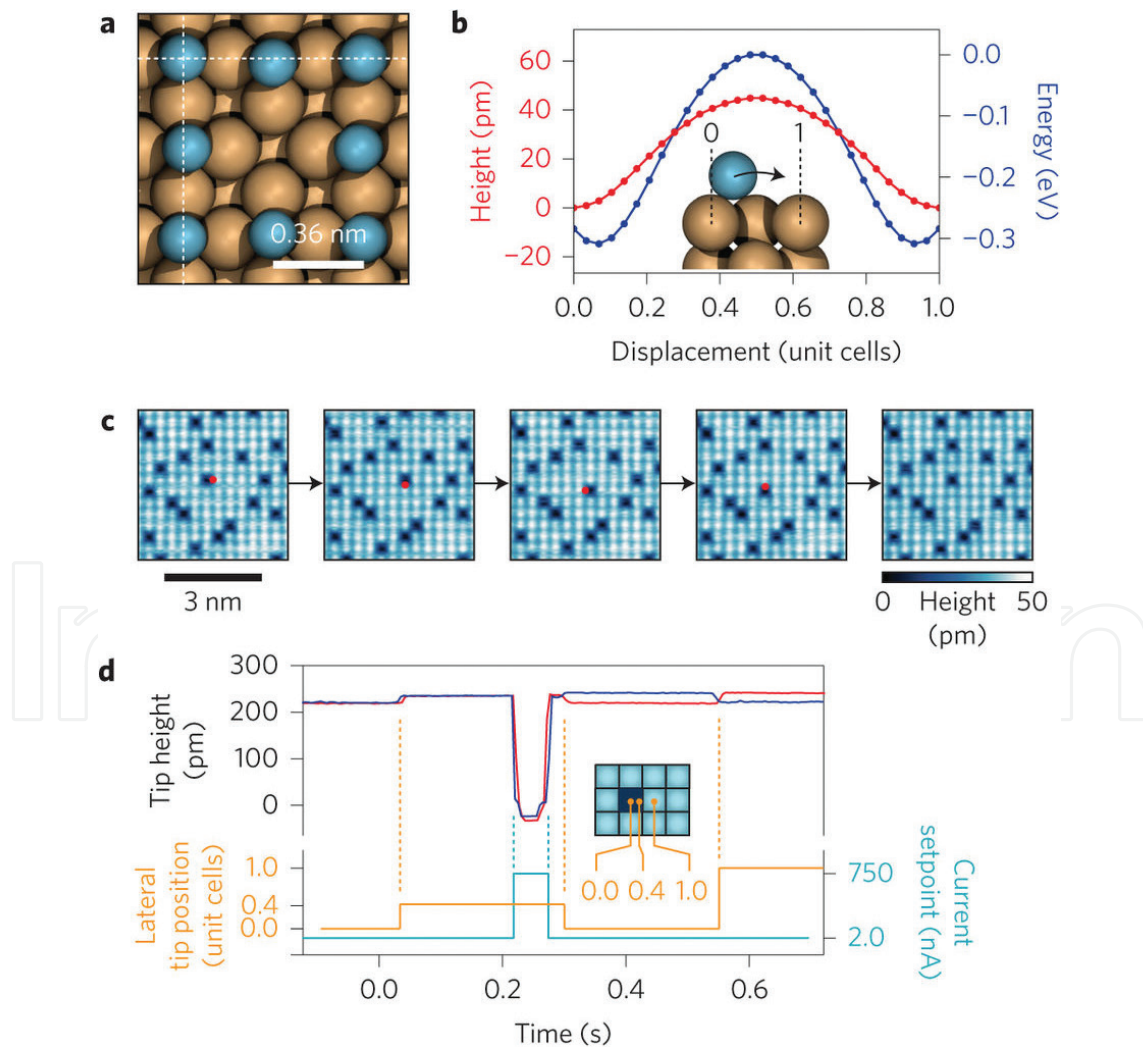


Figure 4. Hopping mechanism of chloride atom vacancy on the chlorinated copper surface (Cu $\langle 100 \rangle$) (Ref. 24). (a) Theoretical atomic structure near a vacancy by density function theory (DFT). Cl atom, Cu atom. (b) Theoretical height profile and potential energy of Cl atom in a switch circle. (c) STM images of consecutive process. (d) Measured tip height in a successful and unsuccessful manipulation.

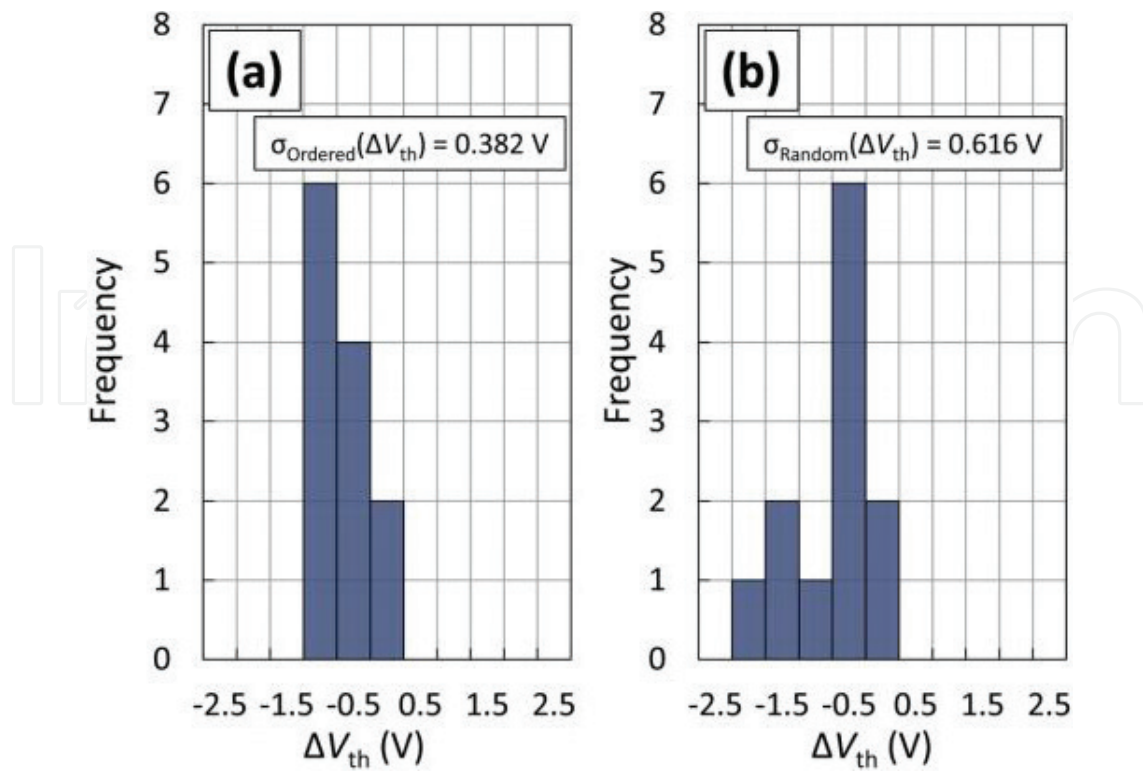


Figure 5. Histograms of voltage shift of (a) ordered array and (b) conventional random dopant distribution (Ref. 31).

The field-effect transistors (FETs) are the workhorse of the microelectronics industry [26]. A decade ago, the channel lengths of FETs were at micrometer level, and the fluctuation of dopants in the bulk device has nearly no impact on the threshold voltage [27, 28]. When the gate length of MOSFET is only ~ 10 nm, the active channel region of devices will only contain several dopants, and the fluctuation in dopant number will generate much stronger random telegraph noise than the average threshold voltage [29] [30]. Ohdomari group reported the phosphorus dopant array [6], As dopant array [31], and other dopants [32] in the silicon devices. It was found that the fluctuation of dopants increases the threshold voltage variation significantly (Figure 5), making the circuitry consisting of these transistors less reliable. This effect will be exacerbated as the transistor size continues to scale down [33]. Consequently, how to precisely control the positions of individual impurities is critical to the reproducibility and reliability of MOSFET circuits.

In conclusion, the individual dopant control is a key to quantum devices. The STM-based atom control and single ion implantation does not meet the industry demand for large-scale fabrication. From the engineering point of view, it is required to develop technologies that can precisely control individual dopants at a large scale.

3. Molecular monolayer doping

Thermal diffusion and ion implantation are the two main doping techniques that are widely used to introduce impurities into semiconductors [34]. By thermal diffusion, the concentration and profile of dopants follow the diffusion equation, which is determined by diffusion

time, temperature, and diffusivity of dopants [35]. The advantage of thermal diffusion is low cost, but it is difficult to obtain shallow junctions due to the fact that dopants are required to be activated at high temperature [36]. The high activation temperature in turn pushes the dopants further into the substrate. Ion implantation and rapid thermal annealing were created to decouple the dopant activation and thermal diffusion of dopants. The depth of dopants is controlled by acceleration voltage and the dopants are activated by rapid annealing temperature. The thermal annealing is accomplished in seconds so that the thermal diffusion of dopants is negligible. Unfortunately, the high-energy ion beam will create a lot of damages to the crystalline lattice [37], which not only amorphizes the silicon surface but also induces defects in bulk.

In 2008, Ho *et al.* [38] reported that the molecular monolayer doping is a potential method to resolve these issues. The monolayer doping protocol consists of two major steps: molecular monolayer formation by hydrosilylation process with dopant-carried precursor molecules (dopant carriers), and rapid thermal annealing (RTA) with a capping layer to block the out-diffusion of dopants. In the first step of self-assembled monolayer on the silicon surface, the density of dopant is determined by the coverage of dopant carrier and molecular size (or footprint). The monolayer is then capped by a thin SiO₂ layer. In the end, dopants are diffused into the silicon shallow surface by RTA process. Through analysis of monolayer doping results under different annealing conditions, the authors found that the depth of diffusion and amount of dopants are determined by both annealing time and temperature [39]. By carefully controlling these parameters, the ultra-shallow junctions were obtained [39].

Since the monolayer doping protocol had been reported, several critical dopants including As, N, Sb, and Bi were performed to control the electronic properties of semiconductor substrate. Here, we would like to discuss in detail the development of monolayer doping in the last decade by different aspects, for example, dopant elements, doping parameters control, and III-V group substrate doping.

a. Dopant elements in monolayer doping

The natural feature of monolayer doping is dopant thermal diffusion, which is originated from precursor molecules on the surface. Silicon is the primary semiconductor material for modern microelectronic industry. Silicon is doped to be n-type by Group V elements and p-type by Group III elements. In Ho's work [38], it was found that the area density of boron is lower than phosphorus, which is caused by significant out-diffusion of boron in SiO₂ capping layer.

Arsenic is also an important donor-type dopant for silicon semiconductor [40]. O'Connell *et al.* [41] reported that As dopants were introduced into silicon surface by using triallylar-sine (TAA) molecules which contain three unsaturated C=C bond. As shown in **Figure 6**, the As-carrying molecules were first anchored on the silicon surface, and As elements were then diffused into the silicon surface with the protection of a capping layer by annealing process. The surface doping concentration reaches to $\sim 2 \times 10^{20} \text{ cm}^{-3}$, and the diffusing depth is $\sim 120 \text{ nm}$ after rapid thermal annealing at 1050°C for 5 s. To investigate the electronic properties after doping process, the authors used a "four point probe test structure" to measure I-V curves for nanowires with different width. The results show that the nanowire conductance is linearly dependent on the nanowire width, implying that the doping is uniform. Moreover, the

cross-sectional transmission electron microscopy (TEM) confirmed that this organic arsenic monolayer doping process will not introduce the lattice damages or crystal defects into the nanowire crystal structure. These results are consistent with other literature reports, such as Ang *et al.* reported [42] the 300 nm level monolayer doping on FIN structure without crystal damage-free.

Another Group V element, nitrogen, is not often used to dope silicon. As reported, nitrogen can decrease the defects and dislocation of silicon crystal, and increase the mechanical strength of silicon [43]. Nitrogen as n-type dopants in silicon has two energy levels at 0.28 and 0.19 eV [44]. However, there is no literature to report the role of nitrogen co-doping with phosphorus in silicon, in particular for the interaction between two dopants. Our group found that nitrogen dopants retard the electrical activity of phosphorus when co-doped with phosphorus via monolayer doping process [45]. As shown in **Figure 7**, nitrogen elements were introduced into the silicon surface by Boc-allylamine or P-N bond with phosphorus. 10-undecenoic molecules that contain the same length of carbon chain were used as a control. Van der Pauw measurements indicate that the sheet resistance of nitrogen-doped silicon is $\sim 35.6 \text{ k}\Omega$, close to the sheet resistance of the N and P co-doped samples. The profile of P and N dopants in the samples is retrieved by secondary ion mass spectroscopy (SIMS) [46]. However, the sheet resistances are not consistent with SIMS data on the assumption of full activation of P dopants, although high activation rates for P dopants in silicon introduced by monolayer doping were reported [39]. To further explore the mechanism of dopants interaction, low temperature Hall measurements were employed to obtain the concentration of dopants that are electrically active. It was found that nitrogen is the key factor to explain these

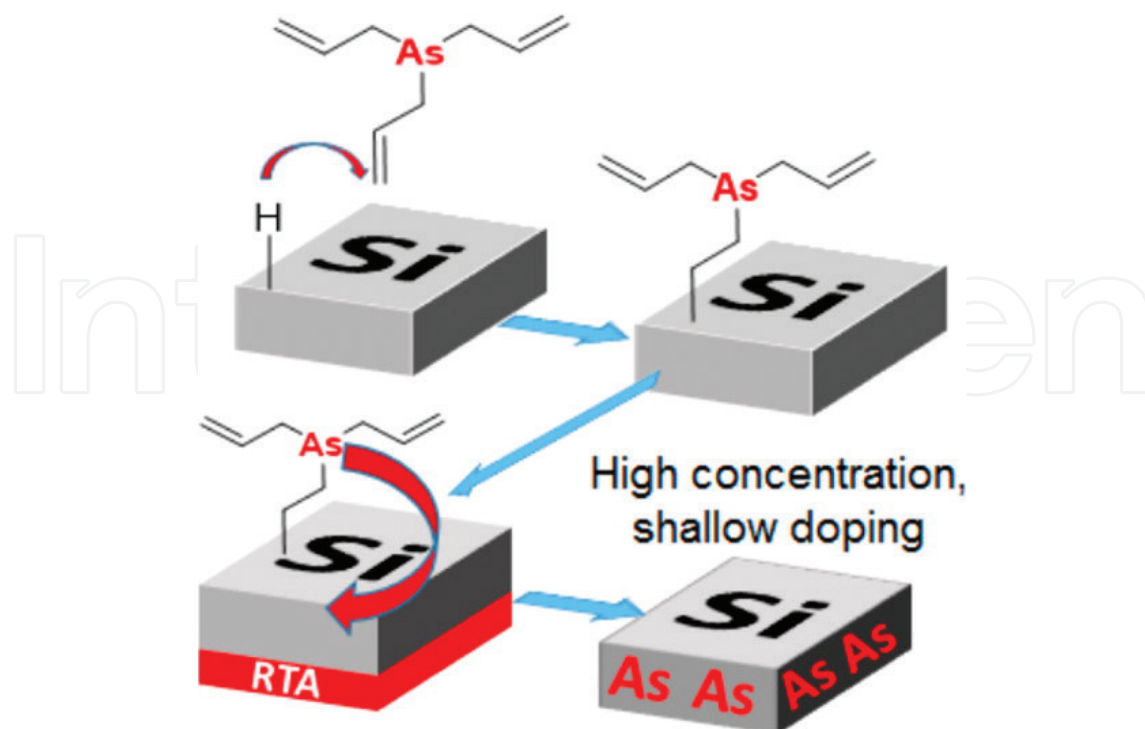


Figure 6. Schematic protocol of organic arsenic monolayer doping process (Ref. 45).

results. When nitrogen was co-doped with phosphorus into silicon, some kind of nitrogen-phosphorus complex entities will form, retarding the electrical activation of phosphorus to ~1%. These results indicate that nitrogen dopants should be avoided to achieve a high activation rate of phosphorus by monolayer doping, although the dopant-carrying molecules that contain nitrogen were used in micelles discrete doping process by Popere *et al.* [47] and anti-oxidation surface with “click” cycloaddition by O’Connell *et al.* [48].

Most monolayer doping processes were performed on the oxide-free Si-H surface. However, the hydrogen-passivated Si surface must be prepared in the glovebox or Schlenk line system, because of the low stability of Si-H in ambient environment and the resultant poor quality of self-assembled monolayer [49]. If the monolayer doping process can be performed on the thin oxide layer of silicon surface, it will simplify the monolayer doping process and find

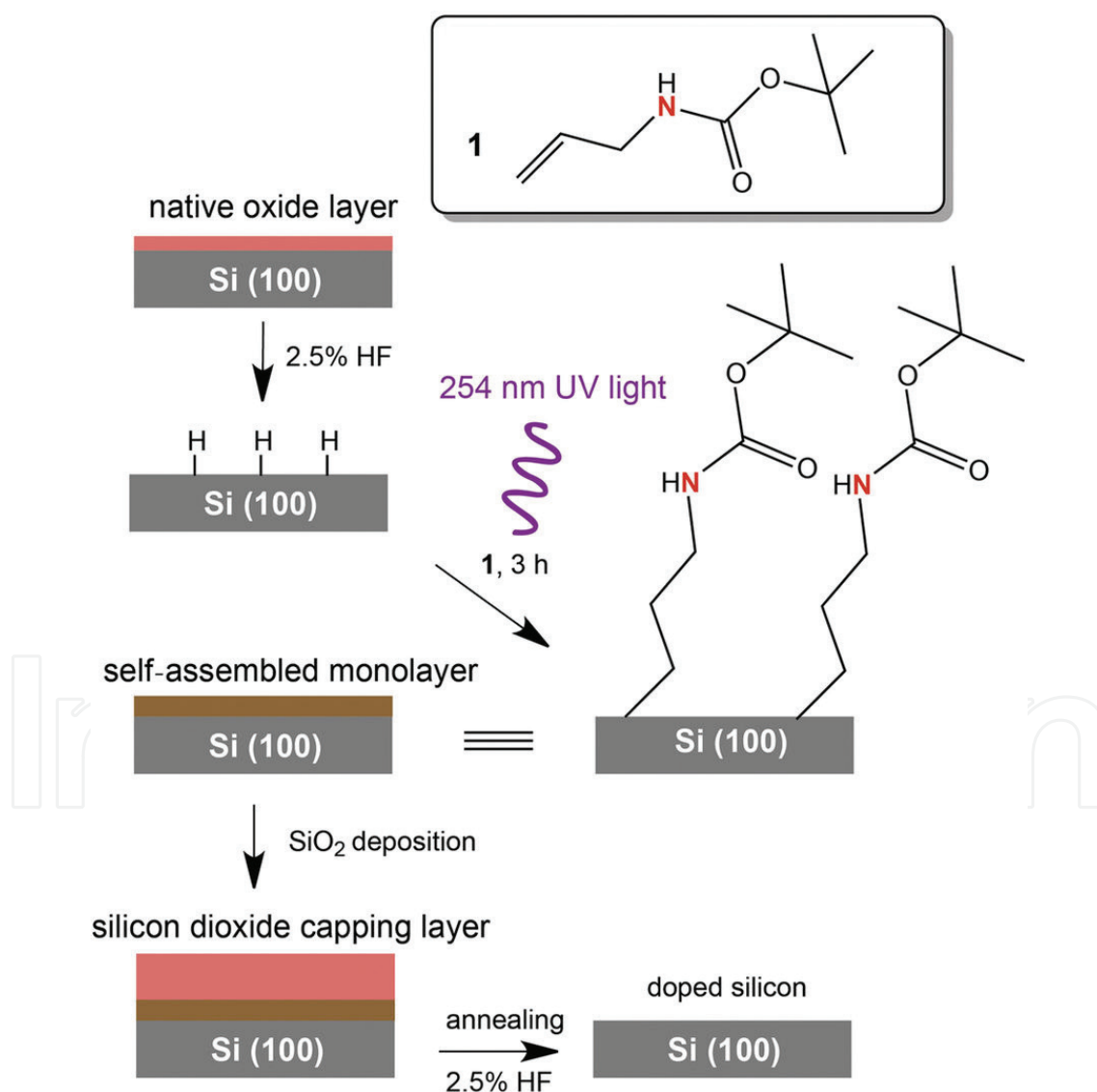


Figure 7. Nitrogen-containing molecule monolayer doping protocol. The small molecules containing nitrogen were anchored on the Si-H surface through the UV initiating method (Ref. 45).

more applications on the silicon devices. Hydrogen silsesquioxane, so-called HSQ as e-beam resist [50], is a series of inorganic Si-O framework compounds with a cubic cage structure. The cage rearrangement will be performed by reacting with phosphoric acid at the Si-O-Si bridge of cage structure [51]. Alphazan *et al.* reported that polyhedral oligomeric silsesquioxane (POSS) (**Figure 8**) carrying phosphorus was grafted onto the oxide-passivated silicon surface [52]. The POSS molecules were synthesized by substitution of phosphoric acid at one site of POSS cage. As shown in **Figure 8**, the POSS molecules were grafted onto the thin oxide layer through the new Si-O-Si bond formation, and POSS with Si-O framework also can be treated as the capping layer instead of coating with an extra SiO₂ layer in the aforementioned doping protocol. The dopants successfully diffused into the silicon surface, and the thin SiO_x layer (0.7 nm) has little impact on the doping process. In addition, this POSS-based monolayer doping on the oxide surface was also used to dope other elements such as antimony in the SiO₂ [53] and Ge substrates [54].

In addition to the applications in nanowire and Fin-structure doping, highly ordered nanopattern doping is another potential application for monolayer doping. In fact, the combination of monolayer doping and nanoimprint lithography is a powerful approach to obtain ordered doping patterns. Based on this technique, Voorthuijzen *et al.* [55] reported two different protocols to attain doped micro-belts by monolayer doping with or without pre-surface monolayer modification process, as shown in **Figure 9**. For the protocol with pre-surface modification, the extra monolayer will be completely removed by O₂ RIE process, while the residual monolayer is under the protection of lithography resist. After RTA process, TOF-SIMS clearly shows the large-scale doping region, indicating that nanoimprint-controlled monolayer doping with ordered patterns is efficient. Moreover, Taheri *et al.* [56] further improved the monolayer pattern doping method by gas-phase monolayer doping, which can achieve smaller doping belt (~2 μm) than nanoimprint-based monolayer pattern doping (~100 μm). The silicon sample with e-beam-lithographic pattern was put into the reactor with gas-phase molecules to obtain the monolayer absorption under a temperature of ~120°C. The gas-phase molecules with unsaturated bonds form stable covalent bonds as the molecules are grafted onto the Si substrate. The width of doping region (~2 μm) and electronic property of the doped micro-belts were confirmed by conductive AFM and I-V measurements, respectively.

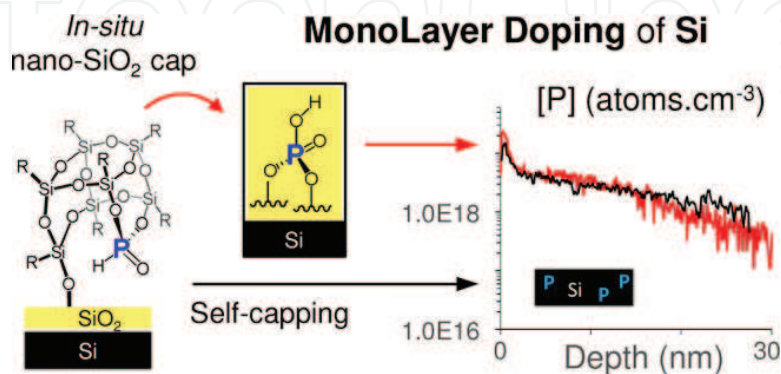


Figure 8. POSS-based monolayer doping process (Ref. 52).

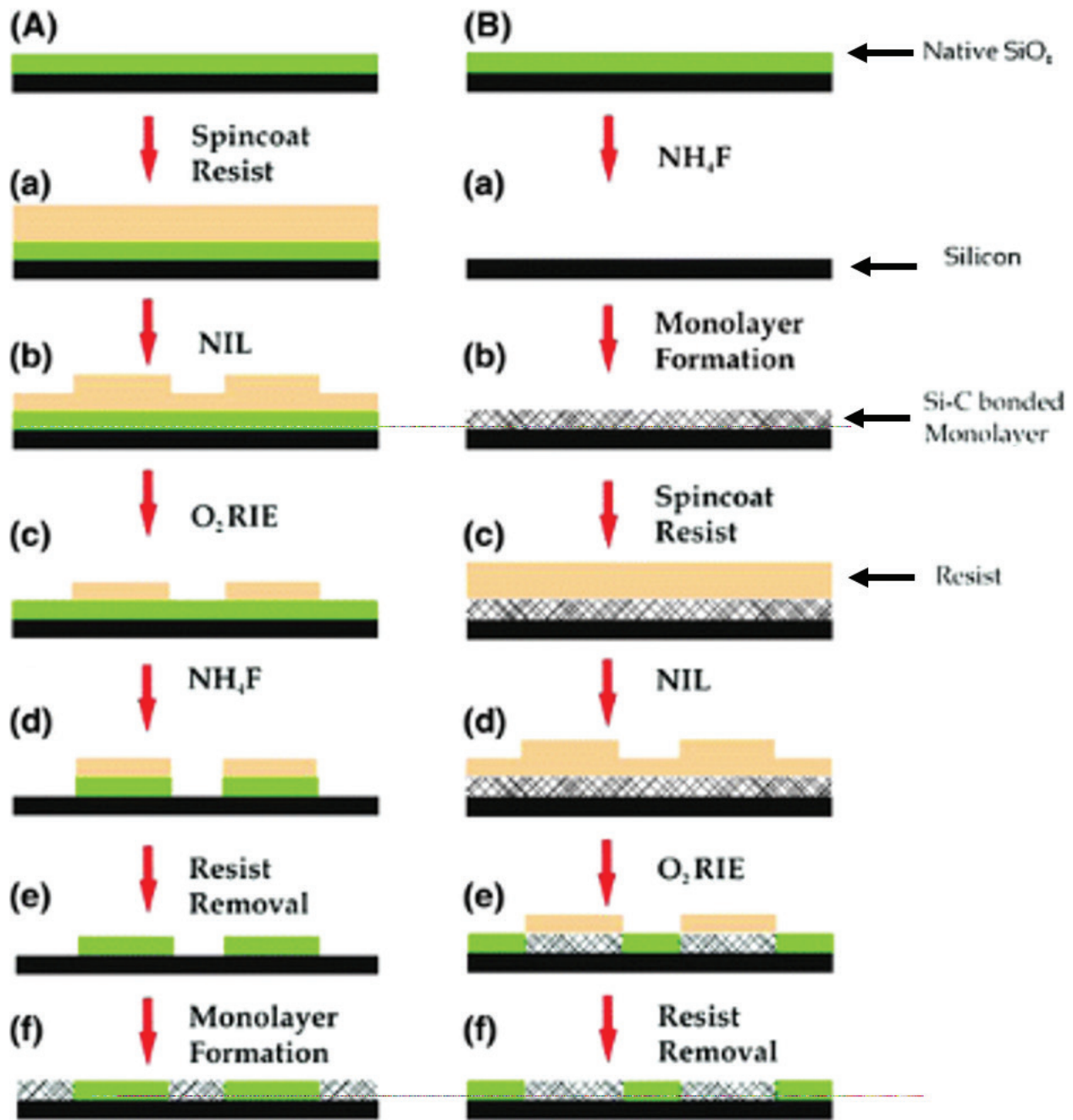


Figure 9. Nanoimprint monolayer doping protocol (Ref. 55). (A) Pattern formation of self-assembled monolayer after nanoimprint process. (B) Pattern formation using nanoimprint and RIE etching. NIL, nanoimprint lithography.

To sum up, we find that the monolayer doping is a potential doping technology for 3D nanodevices at low cost. Owing to the well-developed organic synthesis methods, many dopants can be introduced to different substrates. Nevertheless the monolayer doping process is still under development. More research work is needed on its application particularly in the COMS doping process. [57]

b. Doping concentration control by monolayer doping

Besides the kinds of dopants, the doping concentration is another important factor for the device performance. In Ref. [38], the authors explored the impact of thermal temperature and annealing time on the area doping dose. The control of doping concentration can be also achieved by tuning the molar ratio of dopant-containing molecules and the neutral molecules that do not carry any dopant atoms. The dopant-containing molecules and the neutral molecules are structurally similar, as a result of which similar chemical reactions will occur in the self-assembly process. After the same rapid thermal annealing (RTA) process, the dopant dose show the linear correlation between the rise in sheet resistance and the mixing molar ratio of the dopant-containing molecules to neutral molecules. For example, as the mixing ratio increases from 1:5 to 1:20, the sheet resistance increases from 5 to 20 folds.

Ye *et al.* [58] studied in detail how to control the area doping dose by tuning the mixing ratio of the dilution reagent (1-undecene) and dopant precursors (diethyl vinylphosphonate), as shown in **Figure 10**. After the molecules were grafted to the Si substrate surface, X-ray photoelectron spectroscopy (XPS) was employed to investigate the surface chemistry. The electron energy for different carbon component (C-O vs. C-C, for instance) is different as expected. For example, diethyl vinylphosphonate has two C-O bonds per molecule whereas only C-C bounds exist in the dilution reagent 1-undecene. The ratio of different carbon bonds from XPS allows the authors to derive the ratio of the dilution reagent and dopant precursors that are immobilized on the Si surfaces. As the mixing ratio of dopant precursors increases, the sheet resistance of doped silicon samples significantly decreases. Surprisingly, the surface doping dose is dependent on the mixing ratio in a monomial (instead of linear) correlation as shown in D-SIMS measurements. This phenomenon can be attributed to the difference in reaction efficiency between dopant precursor and diluting reagent.

As mentioned previously, one critical disadvantage of boron monolayer doping is the low doping efficiency (~33%) [38] due to the high diffusivity of boron in SiO₂. The SiO₂ capping layer can effectively block the out-diffusion of phosphorus but less efficiently for boron dopants. This results in a lower doping concentration of boron in silicon. To improve the B doping concentration, one possible solution is to increase the number of boron atoms that each molecule carries. For instance, organoboron or carborane compounds contain a larger amount of boron atoms than the ordinary precursors such as allylboronic acid, pinacol ester, and ABAPE [59]. Ye *et al.* [60] reported that 10-boron carborane (**Figure 11**) was used as the doping precursor to improve the boron doping concentration. The resultant area doping dose reaches $\sim 3 \times 10^{13} \text{ cm}^{-2}$, which is almost 20 times higher than the dose introduced by ABAPE although the number of boron atoms per molecule is only 10 times higher. This is because the footprint of the carborane is relatively smaller when compared to the latter. Clearly, dopant atoms for per footprint area are the critical parameter for doping dose control.

Besides the high area doping dose, the discrete doping also can be prepared by suitable dopant precursors. Micelles, which are micro- or nanoscale globular particles, are prepared by amphiphilic block co-polymers and can carry several guest molecules at the core region. The size selection of micelles is achieved by centrifuging the samples at different speed [61]. Popere *et al.* [62] reported that micelles, which were formed by copolymer polystyrene-block-poly(4-vinylpyridine)

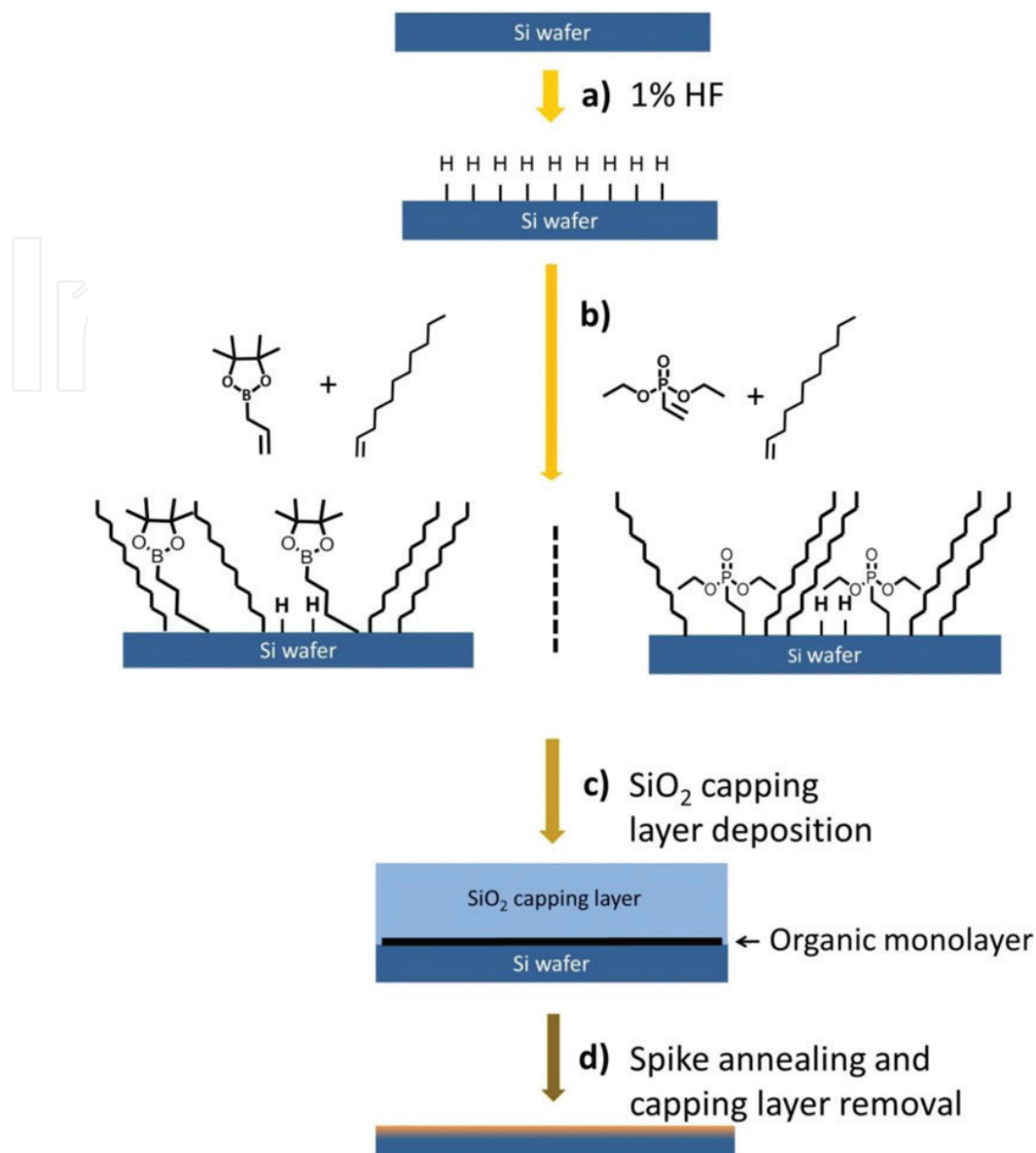


Figure 10. Mixing method to control doping concentration (Ref. 58).

(PS-*b*-P4VP), carried the dopant precursor molecules to prepare the discrete doping. Before the monolayer doping process, the surface morphology was characterized by AFM, confirming that a compact self-assembled film consists of the micelle particles. To check the dopants distribution, the core part of micelles was replaced by HSbF₆ which can be directly observed by transmission electron microscopy (TEM). After the monolayer doping process, the discrete distribution of dopants was indirectly confirmed by TEM.

c. Monolayer doping on III-V semiconductors

Group III-V compounds are direct bandgap semiconductors and often have a much higher electron mobility than silicon [63]. These semiconductors are widely used as light emitting devices (LEDs), lasers, and high-speed transistors. Sulfur is often used as the n-type dopants. For the molecular monolayer doping on Group III-V semiconductors, most attention focuses

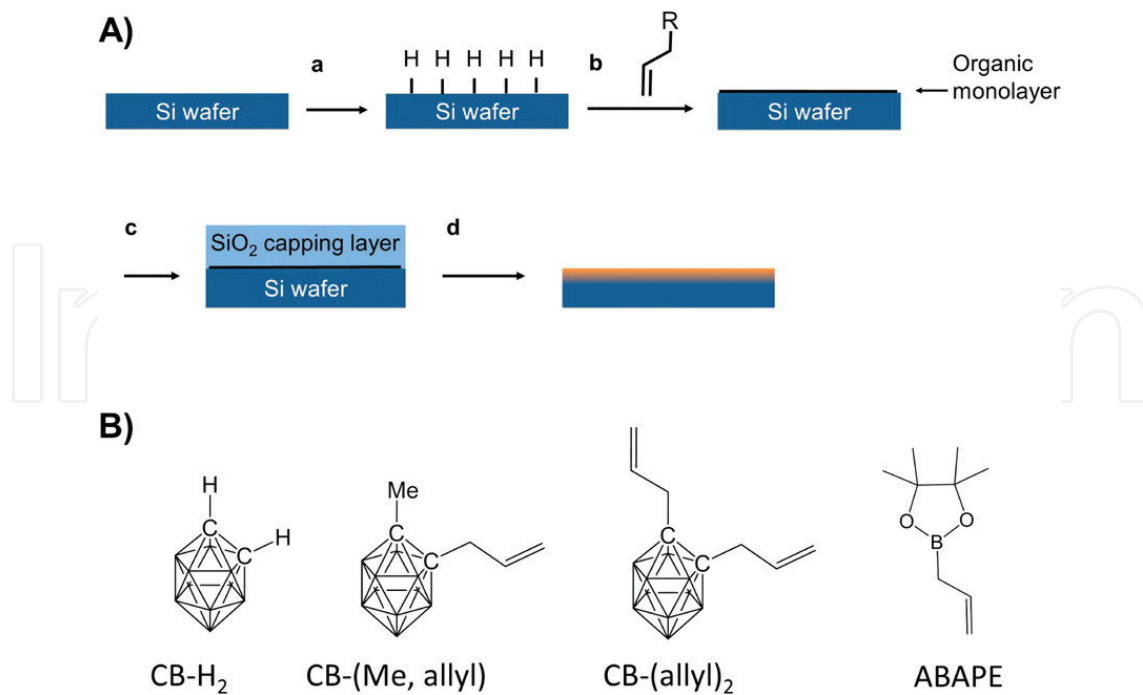


Figure 11. Carborane-based monolayer doping protocol (Ref. 60). (a) Schematic of monolayer doping process. (b) Molecular structure of related-carborane molecules.

on how to obtain high uniform vertical doping profile, for fin structure in particular [64]. The conformal nature of self-assembled monolayers provides the possibility to obtain a uniform doping profile for three dimension structures. Loh *et al.* [65] reported that sulfur-contained inorganic salts (for example, sulfate and sulfite) were applied to dope the InAsGa thin layer. It was found that oxygen atoms in the dopant carrier molecules are of great impact on the doping dose. Cho *et al.* [66] reported later that sulfur was introduced to dope InP. Ho *et al.* [67]

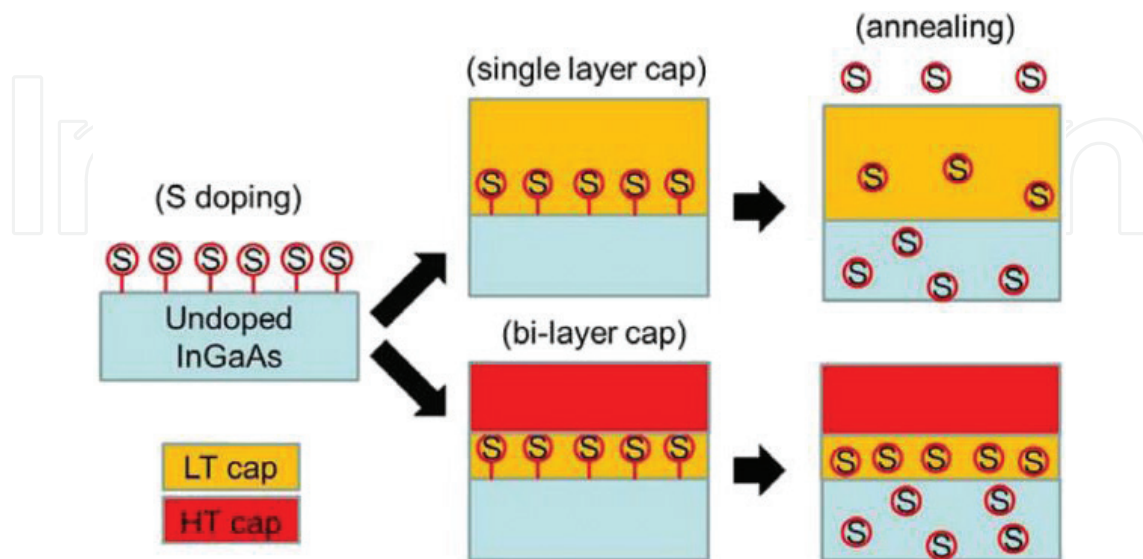


Figure 12. Monolayer doping protocol for group III-V semiconductors (Ref. 68).

reported that ammonium polysulfide was used to dope InAs. To improve the doping dose, Yum *et al.* [68] used a compact capping layer (**Figure 12**) to obtain the higher S doping dose ($1.34 \times 10^{13} \text{ cm}^{-2}$), which is 3 times higher than the previous reports [38]. The knowledge on the molecular monolayer doping on III-V semiconductors is still limited although quite some research works have been conducted on this topic.

d. Impact of other unwanted elements on monolayer doping process

In the self-assembled monolayer doping protocol, the precursors play the essential role to introduce the dopants. However, the dopant precursor molecules also contain other elements such as carbon, oxygen, and hydrogen. These elements other than the desired dopants may

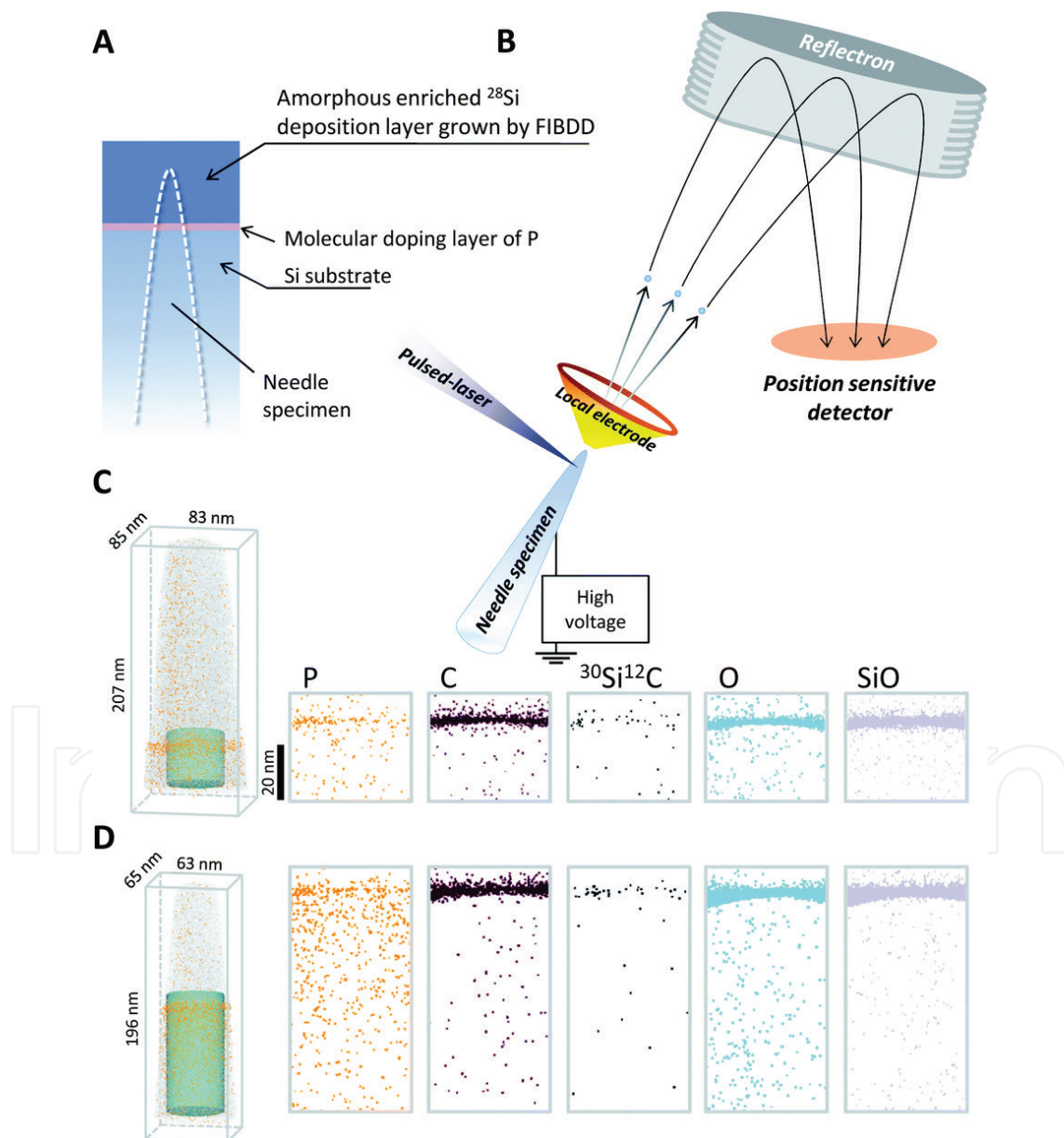


Figure 13. (A) Fabricated specimen by FIB technique. (B) Schematic of APT technique. (C) Elemental distribution of silicon sample annealed by 800 °C and 1025 °C (D), respectively.

have undesired impacts on the electrical properties of the doped devices. Shimizu *et al.* [69] studied the distribution of carbon and other inorganic moieties such as CO, SiO, and O. Laser-assisted atom probe tomography (ATP) was employed to measure the elemental distribution profile. The unwanted diffusion of C- and O-related molecules is revealed, showing that the diffusion of C and O is only limited to the first few atomic layers near the surface. Moreover, the Ar⁺ ion etching results in a different work [70] also indicates the SiC moiety mostly located in the ultra-shallow depth underneath the surface.

However, the effect of unwanted impurities introduced by the monolayer doping process still remains largely unexplored, in particular for carbon and oxygen impurities. In 1960s and 1970s, carbon and oxygen impurities in silicon were the major challenge to develop high-performance integrated circuits. Only when the carbon and oxygen impurities in silicon reduced to a level of 10^{15} cm⁻³ or lower have an era of microelectronics opened. The molecular monolayer doping technique is a promising low-cost doping technique that may potentially replace the traditional ion implantation technology. But it would not happen unless the unwanted carbon and oxygen impurities are removed from the doping process (**Figure 13**).

4. Structural features of dendrimers and dendrimer monolayers

Dendrimers are a series of dendritic molecules containing a core and repeating units. In the past 30 years, the processes for dendrimer synthesis have been well developed. Various dendrimers with different chemical characteristics were synthesized including poly-(amidoamine) with multiple amine-terminated groups [71], polyglycerols with polyetheric chains and hydroxyl groups [72], and silane dendrimers with carboxyl groups [73]. It is relatively easy to synthesize the dendrimers that carry dopant atoms such as phosphorus, sulfur, nitrogen or even iron [74] in addition to carbon, oxygen, and hydrogen. Therefore, dendrimers can be potentially used as precursor molecules for monolayer doping.

Due to their symmetric structure, dendrimers are often in a globular form [75], as shown in **Figure 14**. Previously, we mentioned that periodic discrete doping was achieved by self-assembled micelles. Except for the difference in particle size, dendrimer and micelles are similar in several aspects. For instance, both have moderately rigid structures and their core is both designable. Logically, dendrimers can also be used as dopant precursors or carriers to create discrete doping. In the following, we will discuss in detail the dendrimer synthesis methods and immobilization of dendrimers on silicon surfaces for doping.

According to the literature reports [76], the synthesis strategy of dendrimers can be classified as divergent and convergent growth method as shown in **Figure 15**. In **Figure 15a**, the divergent growth method is initiated from the active sites of core part [77], which is synthesized step-by-step and can obtain the unique molecular weight, such as the highest reported generations (G10) of PAMAM [78]. Another approach is the convergent assembly of well-defined branches to the core [79]. The convergent approach is to generate dendrons which are catenated to the core structure, as shown in **Figure 15b**. It provides a way to control molecular structures and obtain a faster synthesis speed owing to fewer coupling steps and the ability of precisely functionalizing specific growing sites. However, the molecular weight

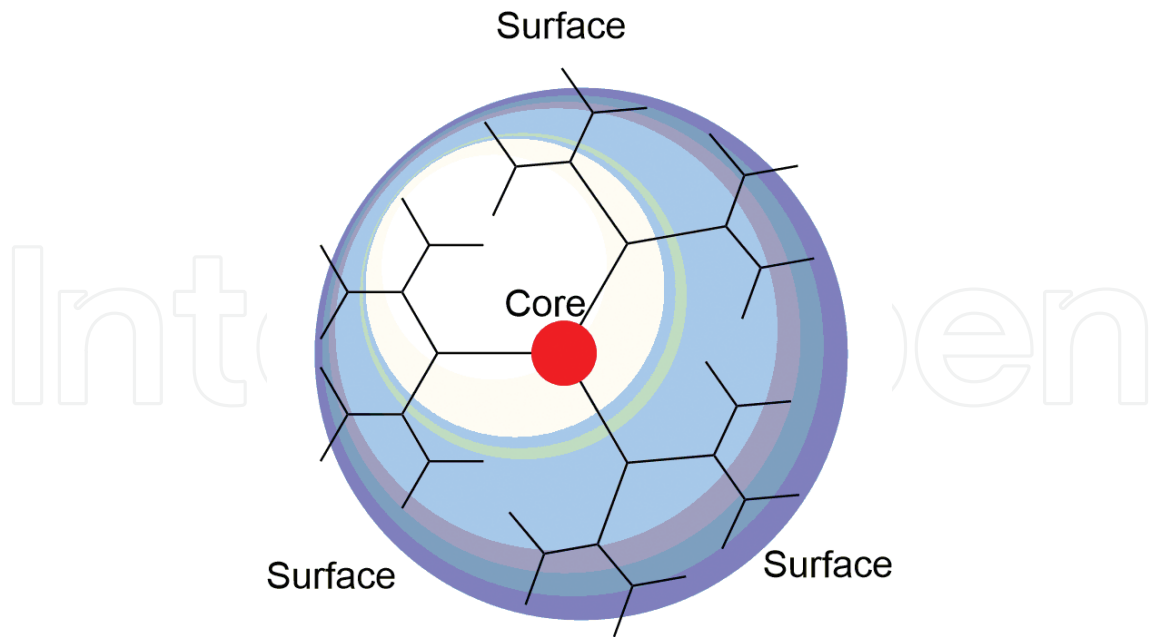


Figure 14. Dendrimer structure containing core and branched units.

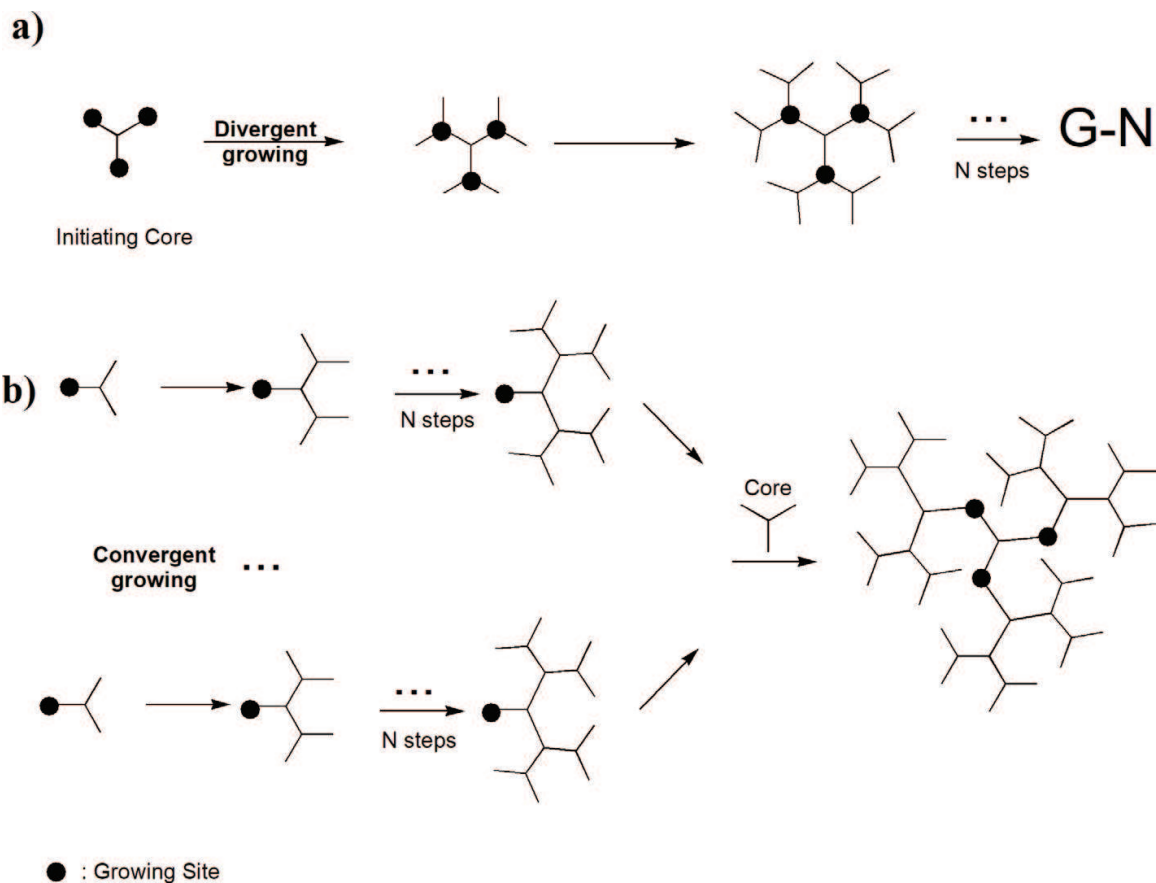


Figure 15. Divergent (a) and convergent growth (b) of dendrimers synthesis.

of dendrimers by convergent methods is smaller than by divergent growth, which is caused by the crowding environment around the core molecules [80]. By using dendrimers as single dopant carriers, it is necessary to ensure that each dendrimer carries only one dopant and the molecular weight is easily controlled from low to high by conventional approaches. Although the convergent method can provide a controlled parallel synthesis route with fewer steps, only the divergent growth can provide a broad range of molecular weight. As a result, we selected the divergent approach as the basic synthesis strategy to generate the dopant carriers.

Polyglycerols are dendrimers in the simplest form. The basic molecular skeleton of polyglycerols is polyetheric chains, and the monomers only contain carbon, oxygen, and hydrogen which are not electrically active in silicon. The excellent water solubility allows polyglycerol molecules to be purified to the CMOS grade using the conventional dialysis in deionized water. In our opinion, polyglycerols are potentially an ideal candidate as dopant carriers.

Depending on the molecular degree of branching, polyglycerols can be classified as dendritic and hyperbranched structures [81]. Dendritic polyglycerols is normally synthesized by the divergent method, as shown in **Figure 16** [72]. The main synthesis steps contain the substitution of 2-propenyl group and formation of vicinal diol moiety by oxidation process (i.e., oxidized by using K_2OsO_4). This synthesis strategy is time-consuming, but the dendritic structure of products is well-defined with unique molecular weight. However, the substitution efficiency decreases as the generation increases. The highest generation with fully dendritic is 5 [82], indicating that it is impossible to synthesize dendritic polyglycerols with very high molecular weight. Unlike time-consuming synthesis of dendritic polyglycerols, hyperbranched polyglycerols (hbPGs) are synthesized by self-polymerization of glycidol monomers at initiating sites. To overcome the drawbacks of the wide molecular weight distribution and the uncontrollable polymerization when using base reagents in earlier studies [83], Sunder *et al.* [84] performed the anionic ring-opening polymerization to obtain the controlled glycidol self-polymerization process, in which the slow addition strategy is adapted to attain a narrow molecular weight distribution. The reported hbPGs molecular weight is typically ranged from 1 to ~7 kDa. The particularly high molecular weight hbPGs can reach up to approximately 25 kDa via the two-step strategy based on the pre-synthesis low molecular weight hbPGs [85]. Meanwhile, Kainthan *et al.* [86] took a different strategy to obtain high molecular weight hbPGs in which dioxane was used as the emulsifying reagent with similar addition strategy. The SEC/MALLS results showed that the molecular weight of hbPGs can achieve to ~700 kDa with low polydispersities (PDI = 1.1–1.3). Besides the synthesis strategy, polyglycerols were synthesized with various initiating cores including tris(hydroxymethyl)-propane [84], graphene [87], and SiO_2 particles [88], implying that hbPGs molecules also can carry different dopants, such as phosphorus, nitrogen, boron, arsenic, iron or even rare earth elements.

Besides the synthesis of polyglycerols as dopant carriers, the graft of polyglycerols onto the substrate surface is another important step for monolayer doping process. Molecules or particles can be grafted onto the solid surface via physical absorption by Van de Waals force, electrostatic interaction or covalent bonds [89]. The physical absorption is weak and the electrostatic interaction is not specific, which, as a result, are not suitable for dopant control. The self-assembly via covalent bonds can generate a stable film for further modification, which

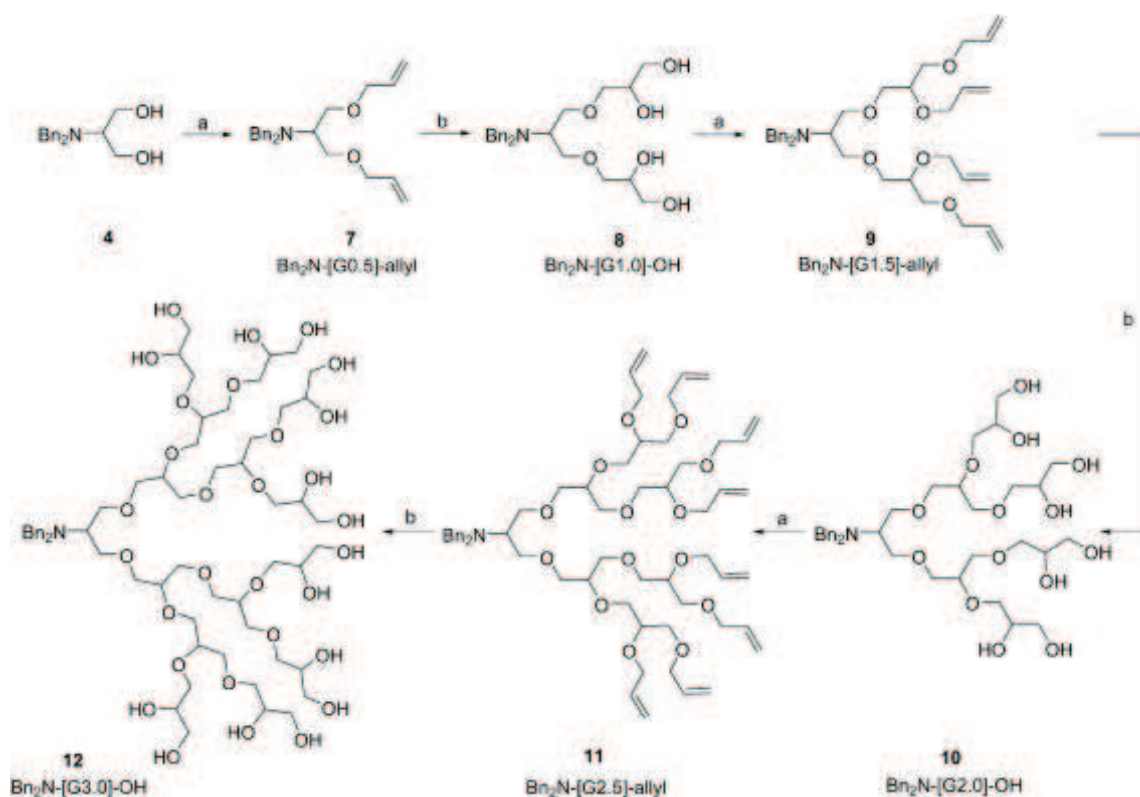


Figure 16. Synthesis flowchart of PG dendrons by substitution and oxidation process (Ref. 72).

is suitable for doping control. In particular, it has been demonstrated that the patterned self-assembled monolayer or ordered lithography patterns with monolayer films can provide ordered and discrete doping patterns [47, 55].

Depending on the order of polymerization and grafting, the graft of polymers can be classified “grafting to” and “grafting from” approaches [90]. As shown in **Figure 17**, the “grafting to” method is to immobilize pre-synthesized polymers or macromolecules onto solid surface. The “grafting from” method is to polymerize on functional surfaces [91]. Ordinary amino-terminated dendrimers are often anchored by covalent bonds with carboxyl groups. For example, Mark *et al.* [92] reported in **Figure 18** that the gold surface was firstly modified by AUT and bis-[sulfosuccinimidyl]suberate molecules through Au-S bonds. Then, through the activated carboxyl by NHS, the G4 dendrimer can be bonded to the carboxyl group by formation of amide bonds.

Polyglycerols contains a large amount of hydroxyl groups mostly located at the molecular surfaces. These hydroxyl groups in return can be modified by other functional groups such as disulfide to bind to gold surface [93]. Although there are few reports on applying the “grafting to” method on silicon surfaces, the well-developed silicon surface chemistry can provide some feasible resolutions to graft hbPGs molecules to, for example, carboxyl-functionalized or halogen-terminated silicon surfaces [49].

Briefly in this section, we discussed in detail the possibility of using molecules as the potential dopant carriers, and the grafting methods of these molecular dopant carriers.

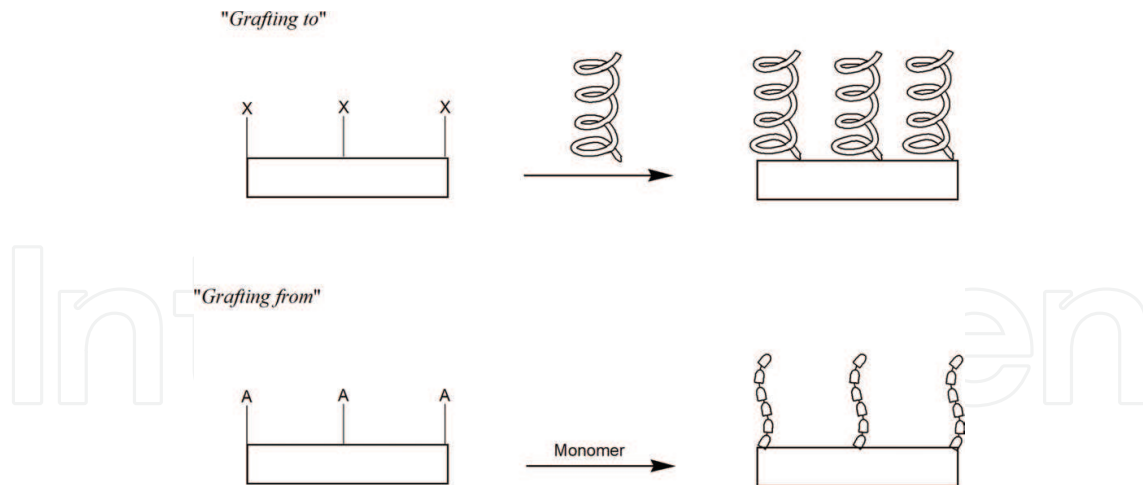


Figure 17. Flowchart of "grafting to" and "grafting from." In figure, X is functional group, and A is initiating site.

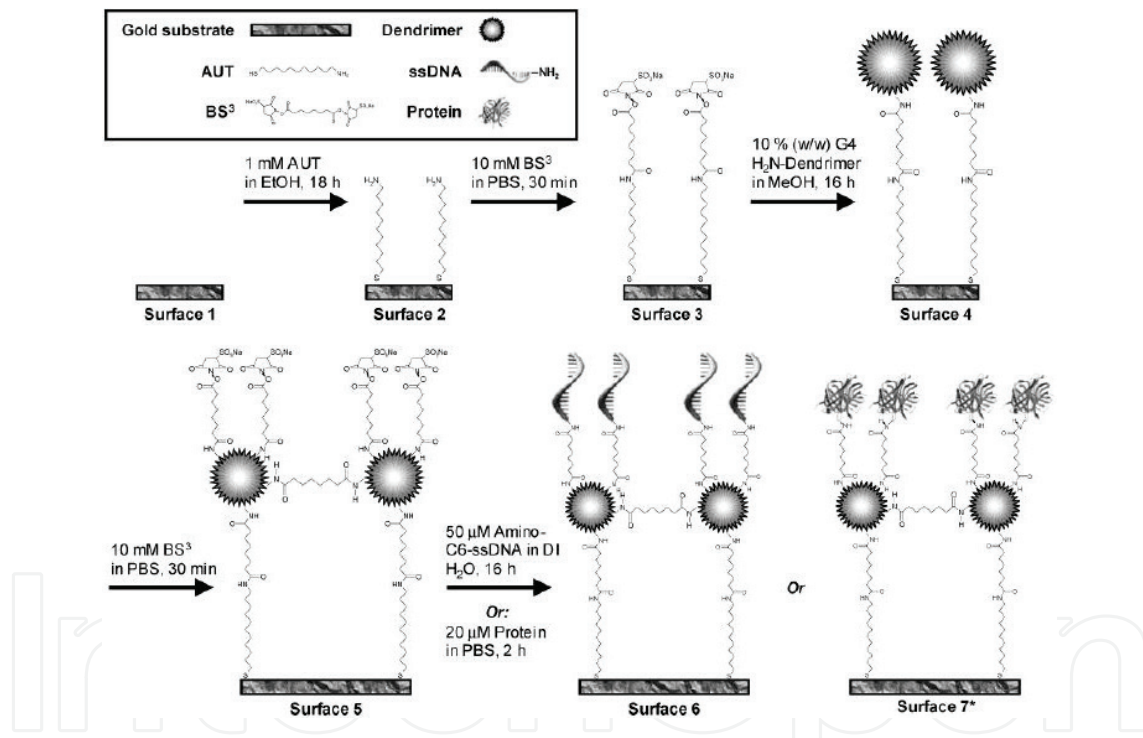


Figure 18. PAMAM G4 was anchored to the carboxyl-terminated gold surface (Ref. 92).

5. Dendrimer-based monolayer doping

hbPGs is an ideal potential candidate as dopant carriers. The molecular size can be readily controlled and the number of dopants that the molecule carries can be precisely tuned. In addition, the unique polymerization process allows the molecules to carry different kinds of dopants. Phosphorus is n-type dopants in silicon [4]. Several research groups have reported the atomic devices based on single phosphorus dopants [4].

Recently, we reported on using hyperbranched polyglycerols (hbPGs) as the phosphorus carriers [10]. The hbPGs were synthesized through the ring-open multibranching polymerization with (tri(4-hydroxyphenyl)phosphine oxide) which is the initiating core. To graft hbPGs onto silicon surfaces, the hydrogen-terminated silicon surfaces were modified with 10-undecenoic acid molecules. The hbPGs were anchored by a process shown in **Figure 19** during which ester bonds are formed. After the rapid annealing process, the phosphorus dopants were diffused into a shallow depth underneath the surface (~ 100 nm) and the areal dose of dopants is approximately $1.64 \times 10^{11} \text{ cm}^{-2}$ with a surface doping concentration of $\sim 10^{17} \text{ cm}^{-3}$. According to the empirical equation [38], the experimental sheet resistance (R_s) would be close to the sheet resistance R_s predicated by SIMS results. However, the actual activation rate evaluated by low temperature Hall measurement is unexpectedly low ($\sim 7\%$) by comparing the electrically active phosphorus dopants with the total phosphorus elements. As our group previously reported [45], nitrogen is one of the factors to retard the activation of phosphorus by forming N-P complex. We believe that the observed low ionization rate is due to nitrogen contamination introduced by coupling reagents (DCC and DMAP) in the reaction process. The XPS full survey and narrow scan also confirmed the nitrogen contamination. Although the final doping efficient of phosphorus is lower than expectation, this protocol confirmed that it is feasible to use dendrimer-like hbPGs molecules as dopant carriers.

Clearly, a nitrogen-free doping process is a must to obtain the highly efficient doping protocol. In the following experiments, we will perform the nitrogen-free and one-step self-assembled monolayer process, which will help us to explore the impact of other elements on the doping efficiency.

Although oxygen and carbon do not electrically dope silicon, they form defects which lower the ionization rate of electrically active dopants by trapping electrons [94]. In the previous studies, different types of carbon-related defects were successfully observed by using deep level transient capacitance spectroscopy (DLTS), for example, interstitial carbon (C_i), interstitial-carbon-substitutional-carbon (C_i-C_s) pairs, and interstitial-carbon-substitutional-phosphorus (C_i-P_s) pairs. These carbon-related defects display different energy levels from 100 to 300 meV [95, 96]. Our group further explored the effect of carbon elements on the doping efficiency by

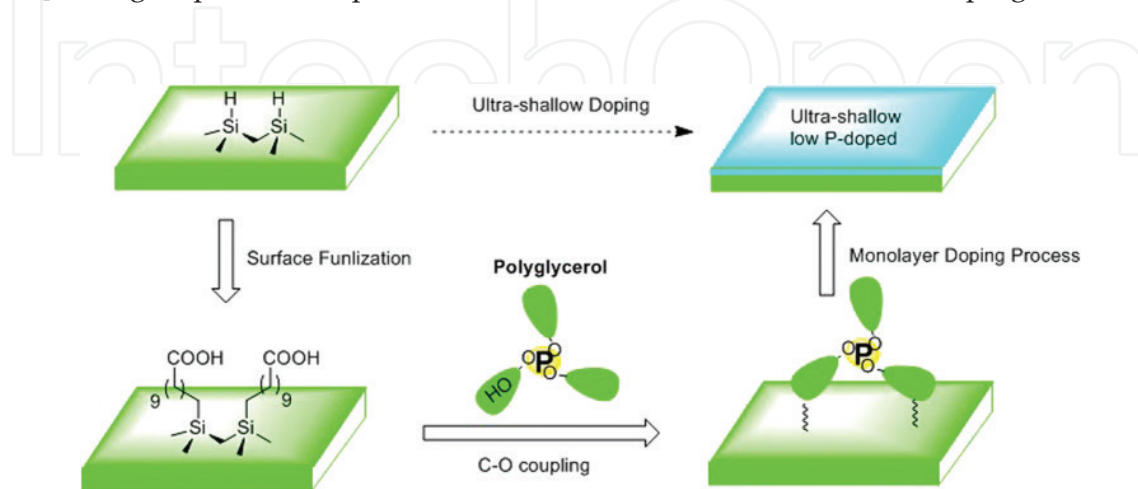


Figure 19. Dendrimer-like macromolecular monolayer doping protocol (Ref. 10).

using DLTS. With the assistance of low temperature Hall measurements, we found that the ionization rate of phosphorus dopants is ~64% when the P concentration is high. This ionization rate is lowered to 10% when the P concentration is low because phosphorus dopants are electrically retarded by the carbon defects by forming interstitial carbon-substitutional phosphorus (C_i-P_s) pairs [95, 97, 98]. Developing techniques to reduce the concentration of carbon impurities introduced by the molecular monolayers is the key to the control of single dopants by the self-assembly of macromolecule dopant carriers.

6. Conclusion

The precise control of individual dopants is critical for the development of single atom electronics and quantum devices. We propose to control single dopant atoms by the self-assembly of individual hbPGs molecules with each carrying one phosphorus atom. Unlike the single atom manipulation techniques by STM and single ion implantation, the dendrimer-based monolayer doping process is more feasible to achieve the controllable doping at large scale from the engineering point of view.

Acknowledgements

This work is supported by the National Science Foundation of China (No. 21503135).

Author details

Haigang Wu^{1,2} and Yaping Dan^{1*}

*Address all correspondence to: yaping.dan@sjtu.edu.cn

1 University of Michigan-Shanghai Jiao Tong University Joint Institute, Shanghai Jiao Tong University, Shanghai, China

2 School of Biomedical Engineering, Shanghai Jiao Tong University, Shanghai, China

References

- [1] Sharma KC, Sharma R, Garg JC. Effect of silver dopant on optical and electrical properties of solution-grown cadmium selenide thin films. *Japanese Journal of Applied Physics*. 1992;**31**(3R):742
- [2] Etemad S, Aspnes D, Kelly M, Thompson R, Tarascon J-M, Hull G. Correlation of dopant-induced optical transitions with superconductivity in $La_{2-x}Sr_xCuO_{4-\delta}$. *Physical Review B*. 1988;**37**(7):3396

- [3] Nakano T, Momono N, Matsuzaki T, Nagata T, Yokoyama M, Oda M, et al. Effects of Zn substitution on magnetic properties and superconductivity in $\text{La}_{2-x}\text{Sr}_x\text{CuO}_4$. *Physica C Superconductivity*. 1999;**317-318**(1):575-578
- [4] Fuechsle M, Miwa JA, Mahapatra S, Ryu H, Lee S, Warschkow O, et al. A single-atom transistor. *Nature Nanotechnology*. 2012;**7**(4):242-246
- [5] Maruyama T, Shiota Y, Nozaki T, Ohta K, Toda N, Mizuguchi M, et al. Large voltage-induced magnetic anisotropy change in a few atomic layers of iron. *Nature Nanotechnology*. 2009;**4**(3):158
- [6] Shinada T, Okamoto S, Kobayashi T, Ohdomari I. Enhancing semiconductor device performance using ordered dopant arrays. *Nature*. 2005;**437**(7062):1128-1131
- [7] Tucker JR, Shen TC. Prospects for atomically ordered device structures based on STM lithography. *Solid-State Electronics*. 1998;**42**(7-8):1061-1067
- [8] Hori M, Shinada T, Ono Y, Komatsubara A, Kumagai K, Tanii T, et al. Impact of a few dopant positions controlled by deterministic single-ion doping on the transconductance of field-effect transistors. *Applied Physics Letters*. 2011;**99**(6):223
- [9] Weber B, Mahapatra S, Ryu H, Lee S, Fuhrer A, Reusch T, et al. Ohm's law survives to the atomic scale. *Science*. 2012;**335**(6064):64-67
- [10] HG W, Guan B, Sun YR, Zhu YP, Dan YP. Controlled doping by self-assembled dendrimer-like macromolecules. *Scientific Reports*. 2017;**7**:41299
- [11] Xie F-Q, Nittler L, Obermair C, Schimmel T. Gate-controlled atomic quantum switch. *Physical Review Letters*. 2004;**93**(12):128303
- [12] Xie FQ, Hüser F, Pauly F, Obermair C, Schön G, Schimmel T. Conductance of atomic-scale Pb contacts in an electrochemical environment. *Physical Review B*. 2010;**82**(7):2283-2288
- [13] Martin CA, Smit RH, van der Zant HS, van Ruitenbeek JM. A nanoelectromechanical single-atom switch. *Nano Letters*. 2009;**9**(8):2940-2945
- [14] Kane BE. A silicon-based nuclear spin quantum computer. *Nature*. 1998;**393**(6681):133-137
- [15] Slichter CP. *Principles of Magnetic Resonance*. New York, USA: Springer Science & Business Media; 2013
- [16] Pla JJ, Tan KY, Dehollain JP, Lim WH, Morton JJ, Zwanenburg FA, et al. High-fidelity readout and control of a nuclear spin qubit in silicon. *Nature*. 2013;**496**(7445):334-338
- [17] Vrijen R, Yablonovitch E, Wang K, Jiang HW, Balandin A, Roychowdhury V, et al. Electron-spin-resonance transistors for quantum computing in silicon-germanium heterostructures. *Physical Review A*. 2000;**62**(1):012306
- [18] Morton JJ, Tyryshkin AM, Brown RM, Shankar S, Lovett BW, Ardavan A, et al. Solid-state quantum memory using the ^{31}P nuclear spin. *Nature*. 2008;**455**(7216):1085-1088
- [19] Tseng GY, Ellenbogen JC. Toward nanocomputers. *Science*. 2001;**294**(5545):1293-1294

- [20] Feynman RP. There's plenty of room at the bottom. *Engineering and science*. 1960;**23**(5):22-36
- [21] Bennewitz R, Crain JN, Kirakosian A, Lin J, McChesney J, Petrovykh D, et al. Atomic scale memory at a silicon surface. *Nanotechnology*. 2002;**13**(4):499
- [22] Kou X, Fan X, Dumas RK, Lu Q, Zhang Y, Zhu H, et al. Memory effect in magnetic nanowire arrays. *Advanced Materials*. 2011;**23**(11):1393-1397
- [23] Schirm C, Matt M, Pauly F, Cuevas JC, Nielaba P, Scheer E. A current-driven single-atom memory. *Nature Nanotechnology*. 2013;**8**(9):645-648
- [24] Kalff F, Rebergen MP, Fahrenfort E, Girovsky J, Toskovic R, Lado JL, et al. A kilobyte rewritable atomic memory. *Nature Nanotechnology*. 2016;**11**(11):926-929
- [25] Maze J, Stanwix P, Hodges J, Hong S, Taylor J, Cappellaro P, et al. Nanoscale magnetic sensing with an individual electronic spin in diamond. *Nature*. 2008;**455**(7213):644-647
- [26] Ferain I, Colinge CA, Colinge J-P. Multigate transistors as the future of classical metal-oxide-semiconductor field-effect transistors. *Nature*. 2011;**479**(7373):310
- [27] Mizuno T, Okamura J-i, Toriumi A, editors. Experimental study of threshold voltage fluctuations using an 8k MOSFET's array. Symposium on VLSI Technology. IEEE Institute of Electrical and Electronics; 1993
- [28] Mizuno T, Okumtura J, Toriumi A. Experimental study of threshold voltage fluctuation due to statistical variation of channel dopant number in MOSFET's. *IEEE Transactions on Electron Devices*. 1994;**41**(11):2216-2221
- [29] Wong H-SP, Taur Y, Frank DJ. Discrete random dopant distribution effects in nanometer-scale MOSFETs. *Microelectronics Reliability*. 1998;**38**(9):1447-1456
- [30] Koenraad PM, Flatté ME. Single dopants in semiconductors. *Nature Materials*. 2011;**10**(2):91
- [31] Hori M, Taira K, Komatsubara A, Kumagai K, Ono Y, Tanii T, et al. Reduction of threshold voltage fluctuation in field-effect transistors by controlling individual dopant position. *Applied Physics Letters*. 2012;**101**(1):013503
- [32] Ohdomari I, Kamioka T. Surface modification of silicon with single ion irradiation. *Applied Surface Science*. 2007;**254**(1):242-246
- [33] Huang W-T, Li Y. Electrical characteristic fluctuation of 16-nm-gate trapezoidal bulk FinFET devices with fixed top-fin width induced by random discrete dopants. *Nanoscale Research Letters*. 2015;**10**(1):116
- [34] Ziegler JF. *Ion Implantation Science and Technology*. Amsterdam, Netherlands: Elsevier; 2012
- [35] Fahey PM, Griffin P, Plummer J. Point defects and dopant diffusion in silicon. *Reviews of Modern Physics*. 1989;**61**(2):289
- [36] Kim K-S, Song Y-H, Park K-T, Kurino H, Matsuura T, Hane K, et al. A novel doping technology for ultra-shallow junction fabrication: Boron diffusion from boron-adsorbed layer by rapid thermal annealing. *Thin Solid Films*. 2000;**369**(1):207-212

- [37] EerNisse E. Sensitive technique for studying ion-implantation damage. *Applied Physics Letters*. 1971;**18**(12):581-583
- [38] Ho JC, Yerushalmi R, Jacobson ZA, Fan Z, Alley RL, Javey A. Controlled nanoscale doping of semiconductors via molecular monolayers. *Nature Materials*. 2008;**7**(1):62
- [39] HoJC, YerushalmiR, SmithG, MajhiP, BennettJ, HalimJ, et al. Wafer-scale, sub-5nm junction formation by monolayer doping and conventional spike annealing. *Nano Letters*. 2009;**9**(2): 725-730
- [40] Pandey K, Erbil A, Cargill G III, Boehme R, Vanderbilt D. Annealing of heavily arsenic-doped silicon: Electrical deactivation and a new defect complex. *Physical Review Letters*. 1988;**61**(11):1282
- [41] O'Connell J, Verni GA, Gangnaik A, Shayesteh M, Long B, Georgiev YM, et al. Organo-arsenic molecular layers on silicon for high-density doping. *ACS Applied Materials & Interfaces*. 2015;**7**(28):15514-15521
- [42] Ang KW, Barnett J, Loh WY, Huang J, Min BG, Hung PY, et al. 300mm FinFET results utilizing conformal, damage free, ultra shallow junctions (X-j similar to 5nm) formed with molecular monolayer doping technique. 2011 Ieee International Electron Devices Meeting (Iedm). 2011
- [43] Imai M, Sumino K. In situ X-ray topographic study of the dislocation mobility in high-purity and impurity-doped silicon crystals. *Philosophical Magazine A*. 1983;**47**(4):599-621
- [44] Tokumaru Y, Okushi H, Masui T, Abe T. Deep levels associated with nitrogen in silicon. *Japanese Journal of Applied Physics Letters*. 1982;**21**(7):L443-L444
- [45] Guan B, Siampour H, Fan Z, Wang S, Kong XY, Mesli A, et al. Nanoscale nitrogen doping in silicon by self-assembled monolayers. *Scientific Reports*. 2015;**5**(12641)
- [46] Sze SM. *Semiconductor Devices: Physics and Technology*. Hoboken, New Jersey, USA: John Wiley & Sons; 2008
- [47] Popere BC, Russ B, Heitsch AT, Trefonas P, Segalman RA. Large-area, Nanometer-scale discrete doping of semiconductors via block copolymer self-assembly. *Advanced Materials Interfaces*. 2016;**2**(18)
- [48] O'Connell J, Collins G, Mcglacken GP, Duffy R, Holmes JD. Monolayer doping of Si with improved oxidation resistance. *ACS Applied Materials & Interfaces*. 2016;**8**(6):4101
- [49] Ciampi S, Harper JB, Gooding JJ. Wet chemical routes to the assembly of organic monolayers on silicon surfaces via the formation of Si-C bonds: Surface preparation, passivation and functionalization. *Chemical Society Reviews*. 2010;**39**(6):2158
- [50] Kupper D, Kupper D, Wahlbrink T, Henschel W, Bolten J, Lemme MC, et al. Impact of supercritical CO₂ drying on roughness of hydrogen silsesquioxane e-beam resist. *Journal of Vacuum Science & Technology B Microelectronics & Nanometer Structures*. 2006;**24**(2):570-574

- [51] Janeta M, John L, Ejfler J, Szafert S. Novel organic-inorganic hybrids based on T8 and T10 silsesquioxanes: Synthesis, cage-rearrangement and properties. *RSC Advances*. 2015;5(88):72340-72351
- [52] Alphazan T, Mathey L, Schwarzwald M, Lin T-H, Rossini AJ, Wischert R, et al. Monolayer doping of silicon through grafting a tailored molecular phosphorus precursor onto oxide-passivated silicon surfaces. *Chemistry of Materials*. 2016;28(11):3634-3640
- [53] Alphazan T, Florian P, Thieuleux C. Ethoxy and silsesquioxane derivatives of antimony as dopant precursors: Unravelling the structure and thermal stability of surface species on SiO₂. *Physical Chemistry Chemical Physics*. 2017;19(12):8595-8601
- [54] Alphazan T, Diaz Alvarez A, Martin F, Grampeix H, Enyedi V, Martinez E, et al. Shallow heavily-doped n⁺⁺ germanium by organo-antimony monolayer doping. *ACS Applied Materials & Interfaces*. 2017
- [55] Voorthuijzen W, Yilmaz MD, Naber WJ, Huskens J, van der Wiel WG. Local doping of silicon using nanoimprint lithography and molecular monolayers. *Advanced Materials* 2011;23(11):1346-1350
- [56] Taheri P, Fahad HM, Tosun M, Hettick M, Kiriya D, Chen K, et al. Nanoscale junction formation by gas-phase monolayer doping. *ACS Applied Materials & Interfaces*. 2017
- [57] O'Connell J, Biswas S, Duffy R, Holmes JD. Chemical approaches for doping nanodevice architectures. *Nanotechnology*. 2016;27(34):342002
- [58] Ye L, Pujari SP, Zuilhof H, Kudernac T, de Jong MP, van der Wiel WG, et al. Controlling the dopant dose in silicon by mixed-monolayer doping. *ACS Applied Materials & Interfaces*. 2015;7(5):3231-3236
- [59] Williams RE. The polyborane, carborane, carbocation continuum: Architectural patterns. *Chemical Reviews*. 1992;92(2):177-207
- [60] Ye L, González-Campo A, Núñez R, de Jong MP, Kudernac T, van der Wiel WG, et al. Boosting the boron dopant level in monolayer doping by Carboranes. *ACS Applied Materials & Interfaces*. 2015;7(49):27357-27361
- [61] Sun JT, Hong CY, Pan CY. Formation of the block copolymer aggregates via polymerization-induced self-assembly and reorganization. *Soft Matter*. 2012;8(30):7753-7767
- [62] Popere BC, Russ B, Heitsch AT, Trefonas P, Segalman RA. Large-area, Nanometer-scale discrete doping of semiconductors via block copolymer self-assembly. *Advanced Materials Interfaces*. 2015;2(18):1500421
- [63] Del Alamo JA. Nanometre-scale electronics with III-V compound semiconductors. *Nature*. 2011;479(7373):317
- [64] Yum JH, Shin HS, Hill R, Oh J, Lee HD, Mushinski RM, et al. A study of capping layers for sulfur monolayer doping on III-V junctions. *Applied Physics Letters*. 2012;101(25):072108-072105

- [65] Loh W-Y, Lee R, Tieckelmann R, Orzali T, Sapp B, Hobbs C, et al., editors. 300mm wafer level sulfur monolayer doping for III-V materials. *Advanced Semiconductor Manufacturing Conference (ASMC), 2015 26th Annual SEMI*; 2015: IEEE
- [66] Cho K, Ruebusch DJ, Lee MH, Moon JH, Ford AC, Kapadia R, et al. Molecular monolayers for conformal, nanoscale doping of InP nanopillar photovoltaics. *Applied Physics Letters*. 2011;**98**(20):203101
- [67] Ho JC, Ford AC, Chueh YL, Leu PW, Ergen O, Takei K, et al. Nanoscale doping of InAs via sulfur monolayers. *Applied Physics Letters*. 2009;**95**(7):072108-072103
- [68] Yum J, Shin H, Hill R, Oh J, Lee H, Mushinski RM, et al. A study of capping layers for sulfur monolayer doping on III-V junctions. *Applied Physics Letters*. 2012;**101**(25):253514
- [69] Shimizu Y, Takamizawa H, Inoue K, Yano F, Nagai Y, Lamagna L, et al. Behavior of phosphorous and contaminants from molecular doping combined with a conventional spike annealing method. *Nanoscale*. 2014;**6**(2):706-710
- [70] Pillers MA, Lieberman M. Embedded silicon carbide “replicas” patterned by rapid thermal processing of DNA origami on silicon. *Journal of Vacuum Science & Technology B, Nanotechnology and Microelectronics: Materials, Processing, Measurement, and Phenomena*. 2016;**34**(6):060602
- [71] Ferruti P, Marchisio MA, Duncan R. Poly (amido-amine) s: Biomedical applications. *Macromolecular Rapid Communications*. 2002;**23**(5-6):332-355
- [72] Wyszogrodzka M, Möws K, Kamlage S, Wodzińska J, Plietker B, Haag R. New approaches towards monoamino polyglycerol dendrons and dendritic triblock amphiphiles. *European Journal of Organic Chemistry*. 2008;**2008**(1):53-63
- [73] Boisselier E, Ornelas C, Pianet I, Aranzaes JR, Astruc D. Four generations of water-soluble Dendrimers with 9 to 243 benzoate tethers: Synthesis and dendritic effects on their ion pairing with acetylcholine, Benzyltriethylammonium, and dopamine in water. *Chemistry-A European Journal*. 2008;**14**(18):5577-5587
- [74] Kim C, Park E, Song CK, Koo BW. Ferrocene end-capped dendrimer: Synthesis and application to CO gas sensor. *Synthetic metals*. 2001;**123**(3):493-496
- [75] Tokuhisa H, Kubo T, Koyama E, Hiratani K, Kanesato M. A new method to fabricate single-molecule Nanoarrays using Dendrimer-based templates. *Advanced Materials*. 2003;**15**(18):1534-1538
- [76] Ooya T, Lee J, Park K. Hydrotropic dendrimers of generations 4 and 5: Synthesis, characterization, and hydrotropic solubilization of paclitaxel. *Bioconjugate Chemistry*. 2004;**15**(6):1221-1229
- [77] Brauge L, Magro G, Caminade A-M, Majoral J-P. First divergent strategy using two AB₂ unprotected monomers for the rapid synthesis of dendrimers. *Journal of the American Chemical Society*. 2001;**123**(27):6698-6699

- [78] Hedden RC, Bauer BJ, Smith AP, Gröhn F, Amis E. Templating of inorganic nanoparticles by PAMAM/PEG dendrimer–star polymers. *Polymer*. 2002;**43**(20):5473-5481
- [79] Miller TM, Neenan TX. Convergent synthesis of monodisperse dendrimers based upon 1, 3, 5-trisubstituted benzenes. *Chemistry of Materials*. 1990;**2**(4):346-349
- [80] Holister P, Vas CR, Harper T. Dendrimers. *Technology white papers*. 2003;**6**:1-15
- [81] Calderón M, Quadir MA, Sharma SK, Haag R. Dendritic polyglycerols for biomedical applications. *Advanced Materials*. 2010;**22**(2):190-218
- [82] Haag R, Sunder A, Stumbé J-F. An approach to glycerol dendrimers and pseudo-dendritic polyglycerols. *Journal of the American Chemical Society*. 2000;**122**(12):2954-2955
- [83] Sandler SR, Berg FR. Room temperature polymerization of glycidol. *Journal of Polymer Science Part A: Polymer Chemistry*. 1966;**4**(5):1253-1259
- [84] Sunder A, Hanselmann R, Frey H, Mülhaupt R. Controlled synthesis of hyperbranched polyglycerols by ring-opening multibranching polymerization. *Macromolecules*. 1999;**32**(13):4240-4246
- [85] Wilms D, Wurm F, Jr N, Böhm P, Kemmer-Jonas U, Frey H. Hyperbranched polyglycerols with elevated molecular weights: A facile two-step synthesis protocol based on polyglycerol macroinitiators. *Macromolecules*. 2009;**42**(9):3230-3236
- [86] Kainthan RK, Muliawan EB, Hatzikiriakos SG, Brooks DE. Synthesis, characterization, and viscoelastic properties of high molecular weight hyperbranched polyglycerols. *Macromolecules*. 2006;**39**(22):7708-7717
- [87] Sui K, Zhang Q, Liu Y, Tan L, Liu L. Improved interfacial and impact properties of carbon fiber/epoxy composites through grafting hyperbranched polyglycerols on a carbon fiber surface. *E-Polymers*. 2014;**14**(2):145-150
- [88] Khan M, Huck WT. Hyperbranched polyglycidol on Si/SiO₂ surfaces via surface-initiated polymerization. *Macromolecules*. 2003;**36**(14):5088-5093
- [89] Rajca A. An introduction to ultrathin organic films: From Langmuir-Blodgett to self-assembly. *Advanced Materials*. 2010;**4**(4):309
- [90] Minko S. Grafting on solid surfaces: “grafting to” and “grafting from” methods. *Polymer surfaces and interfaces*: Springer. 2008:215-234
- [91] Stamm M. Polymer surfaces and interfaces. *Polymer Surfaces and Interfaces: Characterization, Modification and Applications*. Berlin, Germany: Springer Berlin Heidelberg; 2008;1. ISBN 978-3-540-73864-0
- [92] Mark SS, Sandhyarani N, Zhu C, Campagnolo C, Batt CA. Dendrimer-functionalized self-assembled monolayers as a surface plasmon resonance sensor surface. *Langmuir*. 2004;**20**(16):6808-6817

- [93] CS D-C, Biesalski M, Dr RH. Self-assembled monolayers of dendritic Polyglycerol derivatives on gold that resist the adsorption of proteins. *Chemistry-A European Journal*. 2004;**10**(11):2831-2838
- [94] Stavola M, Pearton SJ, Davies G. *Defects in Electronic Materials*. Pittsburgh, PA: Materials Research Society; 1988
- [95] Zhan XD, Watkins GD. Electron paramagnetic resonance of multistable interstitial-carbon–substitutional-group-V-atom pairs in silicon. *Physical Review B Condensed Matter*. 1993;**47**(11):6363
- [96] Song LW, Benson BW, Watkins GD. Identification of a bistable defect in silicon: The carbon interstitial-carbon substitutional pair. *Applied Physics Letters*. 1987;**51**(15):1155-1157
- [97] Song L, Watkins G. EPR identification of the single-acceptor state of interstitial carbon in silicon. *Physical Review B*. 1990;**42**(9):5759
- [98] Gao XJ, Guan B, Mesli A, Chen KX and Dan YP. Deep level transient spectroscopic investigation of phosphorus-doped silicon by self-assembled molecular monolayers. Under review in *Nature Communications*

